Design and Synthesis of P1−P3 Macrocyclic Tertiary-Alcohol-Comprising HIV-1 Protease Inhibitors

Advait Joshi,[†,‖] Jean-Baptiste Véron,[†,‖] Johan Unge,[‡] Åsa Rosenquist,[§] Hans Wallberg,[§] Bertil Samuelsson,[§] Anders Hallberg,[†] and Mats Larhed*,[†]

[†]Department of Medicinal Chemistry, Organic Pharmaceutical Chemistry, BMC, Uppsala University, P.O. Box 574, SE-751 23 Uppsala, Sweden

[‡]MAX IV-laboratory, Lund University, P.O. Box 118, SE-221 00 Lund, Sweden

[§]Medivir AB, P.O. Box 1086, SE-141 22 Huddinge, Sweden

Ⓢ Supporting Information

ABSTRACT: To study P1−P3 macrocyclizations of previously reported tertiary-alcohol-comprising HIV-1 protease inhibitors (PIs), three new 14- and 15-member macrocyclic PIs were designed, synthesized by ring-closing metathesis, and evaluated alongside with 10 novel linear PIs. Cocrystallized complexes of the macrocyclic PIs and the HIV-1 protease are presented, analyzed, and discussed. The macrocyclic structures exhibited higher activities than the linear precursors with K_i and EC_{50} values down to 3.1 nM and 0.37 μM, respectively.

$EC_{50} = 0.37\ \mu M$; $K_i = 3.1$ nM
$CC_{50} > 50\ \mu M$

INTRODUCTION

HIV-1 protease inhibitors (PIs) are essential components in highly active antiretroviral therapy (HAART) but are associated with severe side effects such as dyslipidaemia, hypersensitivity, and lipodystrophy.[1,2] As a consequence, poor patient compliance is commonly observed. There are nine HIV-1 protease inhibitors in the clinic,[3,4] and, with one exception,[5] these comprise inert bioisosteres mimicking the transition state of the peptide-bond cleavage site of the gag and gag−pol precursor polyproteins. The PIs bind competitively to the active site of the protease and coordinate with the flaps in a closed position via a structural water molecule.[6,7] Unfortunately, the inherent peptidic character of these inhibitors results in their having low aqueous solubility, poor membrane permeability, high protein binding, and often low bioavailability after oral administration.[6,7] Therefore, high doses are generally needed. Furthermore, the development of resistance toward many of the drugs used today is an emerging concern.[8,9] Atazanavir (Figure 1) presents a high oral bioavailability and was the first PI that was approved for once-daily administration.[10,11] This inhibitor shows a distinct resistance profile from others PIs such as, for example, the characteristic mutation I50L that reduce susceptibility to atazanavir but increases susceptibility to other PIs.[12,13]

Considering the fast development of resistant viral strains in general,[12] there is a need for new, unique structural entities that could provide alternatives for use in future anti-HIV pharmacotherapy.

A secondary alcohol is a characteristic feature in the transition-state isosters of the PIs in clinic (e.g., atazanavir).

Figure 1. Atazanavir.

We have reported series of potent HIV-1 PIs with the general formula shown in Figure 2[14−20] related to both atazanavir and indinavir but encompassing a shielded tertiary alcohol as part of the transition-state-mimicking scaffold and different lengths of the central carbon spacer ($n = 1−3$). Previously, only a few examples were reported where tertiary alcohols were used as part of transition-state mimics in aspartyl PIs.[21,22] Despite an unsymmetrical arrangement of the tertiary alcohol over the catalytically active aspartic acid residues, the tertiary-alcohol-comprising HIV-1 PIs furnished high enzyme activity as well as excellent permeation through Caco-2 cell membranes.[14−20] Unfortunately, the compounds with a one carbon tether ($n = 1$) provided only moderate cell activity.[14−16]

Encouraged by the often positive pharmacokinetic and pharmacodynamic outcome after various macrocyclizations of linear bioactive compounds,[23,24] we have now applied this
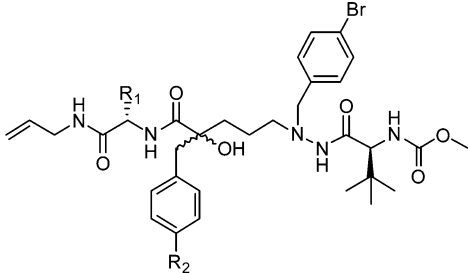
Figure 2. (a) Generic structure of a linear HIV-1 protease inhibitor with a tertiary-alcohol-containing transition-state mimic ($n = 1-3$). (b) Generic structure of the new P1−P3 cyclized tertiary-alcohol-containing HIV-1 protease inhibitors ($n = 3$).

Table 1. Enzyme Inhibition Data, Antiviral Activity, and Cytotoxicity of Noncyclic Tertiary-Alcohol-Comprising HIV-1 PIs

cmpd	R_1	R_2	K_i (nM)	EC_{50} (μM)	CC_{50} (μM)	P_{app} ($\times 10^{-6}$ cm/s)
(R)-14a	i-Pr	Br	11	5.8	22	
(R)-14b	t-Bu	Br	10	2.9	29	
(R)-15a	i-Pr	vinyl	15	6.9	25	
(R)-15b	t-Bu	vinyl	16	5.3	44	45[a]
(R)-16a	i-Pr	allyl	30	6.0	24	44[a], 16[b]
(R)-16b	t-Bu	allyl	37	7.5	>50	44[a], 85[b]
(S)-14a	i-Pr	Br	1000	>50	4.5	
(S)-14b	t-Bu	Br	980	>50	21	
(S)-15a	i-Pr	vinyl	780	>50	5.8	
(S)-15b	t-Bu	vinyl	720	>50	25	

[a]Measured Caco-2 permeabilities. [b]Predicted Caco-2 permeabilities with the program QikProp (Schrödinger).

Scheme 1[a]
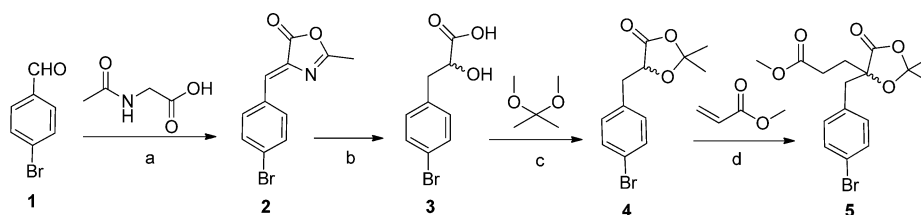
[a]Reagents and conditions: (a) sodium acetate, acetic anhydride, 120 °C, 4 h, 89%; (b) (1) HCl 3N, 120 °C, 24 h, (2) Zn/Hg, toluene, 120 °C, 5 h, 83%; (c) PPTS, CHCl$_3$, 70 °C, 4 h, 84%; (d) (1) LDA, −78 °C, THF, (2) methyl acrylate, −78 °C, 30 min, 54%.

strategy and utilized the ruthenium-catalyzed metathesis reaction for the ring-closing reaction of a series of tertiary-alcohol-based HIV PIs. Calculations in QikProp (Schrödinger) provided high predicted Caco-2 permeabilities for cyclized tertiary-alcohol-containing HIV-1 protease inhibitors (Tables 1 and 2). Although the macrocyclization strategy has been previously investigated for the design of improved HIV-1 PIs,[25−28] no example of macrocyclic tertiary alcohols have been reported. We herein report the synthesis and biological evaluation of a series of 14- and 15-member P1−P3 macrocycles encompassing a tertiary alcohol in the transition-state-mimicking scaffold.

■ CHEMISTRY

Commercially available *para*-bromobenzaldehyde **1** was condensed with *N*-acetylglycine, and the resulting oxazolone **2** was then reduced by HCl/amalgamated zinc. Diol **3** obtained was protected using 2,2-dimethoxypropane to yield **4** followed by a LDA-mediated conjugate addition with methyl acrylate, providing aryl bromide **5** (Scheme 1).

Compounds **8a−b** were prepared in two steps from Boc-L-valine **6a** or Boc-Tle-OH **6b** coupled with allylamine before the removal of the Boc group with TFA. Treatment of methyl ester **5** by TFA in H$_2$O resulted in hydrolysis and subsequent intramolecular lactonisation. The liberated carboxylic acid

Scheme 2[a]
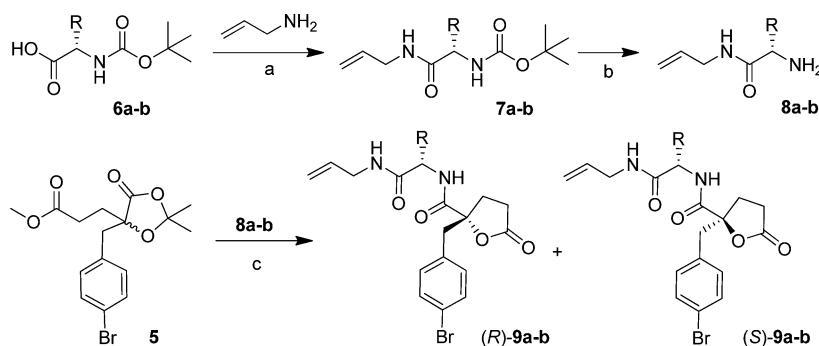
[a]Reagents and conditions: (a) **6a** (R = *i*Pr) or **6b** (R = *t*Bu), allylamine, HOBt, EDC, 4-methylmorpholine, DCM, rt, 15 h, 92%; (b) TFA, DCM, rt, 1 h; (c) (1) TFA, H$_2$O, 80 °C, 15 h, (2) compound **8a** or **8b**, HOBt, EDC, 4-methylmorpholine, DCM, rt, 15 h, (*R*)-**9a–b** 41–44%, (*S*)-**9a–b** 41–44%.

Scheme 3[a]
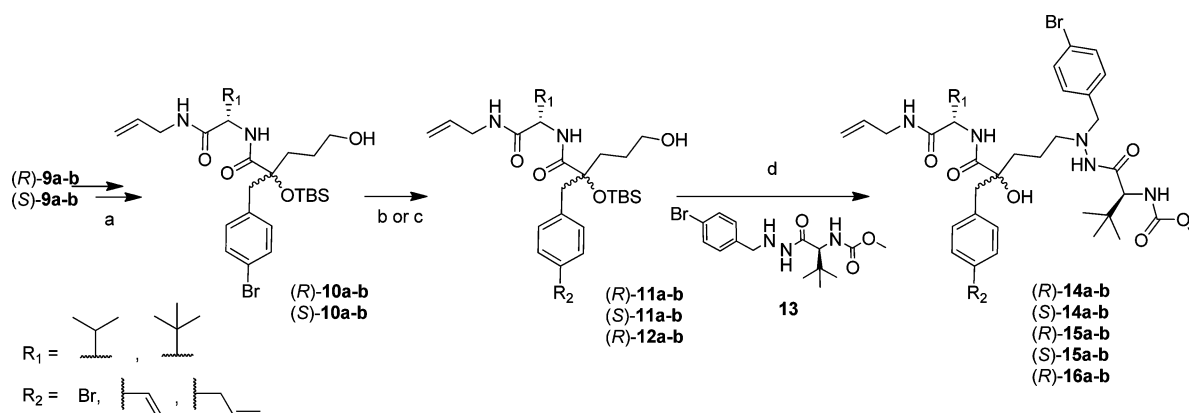
[a]Reagents and conditions: (a) (1) LiBH$_4$, THF, rt, 15 h; (2) pivaloyl chloride, pyridine, DCM, rt, 15 h; (3) TBSOTf, Et$_3$N, DCM, rt, 15 h; (4) LiBH$_4$, THF, rt, 15 h, four steps: 42–45%; (b) 2,4,6-trivinylcyclotriboroxane pyridine complex, Pd(OAc)$_2$, HP(*t*Bu)$_3$BF$_4$, potassium carbonate, DME, H$_2$O, MW, 100 °C, 30 min, 81–97%; (c) allyltributylstannyl, Pd(PPh$_3$)$_2$Cl$_2$, CuO, DMF, MW, 150 °C, 30 min, 5–-62%; (d) (1) Dess–Martin periodinane, DCE, (2) compound **13**, sodium triacetoxyborohydride, DCE, 15 h; (3) TBAF, THF, 0 °C to rt, 30 min, three steps: 25–56%.

Scheme 4[a]
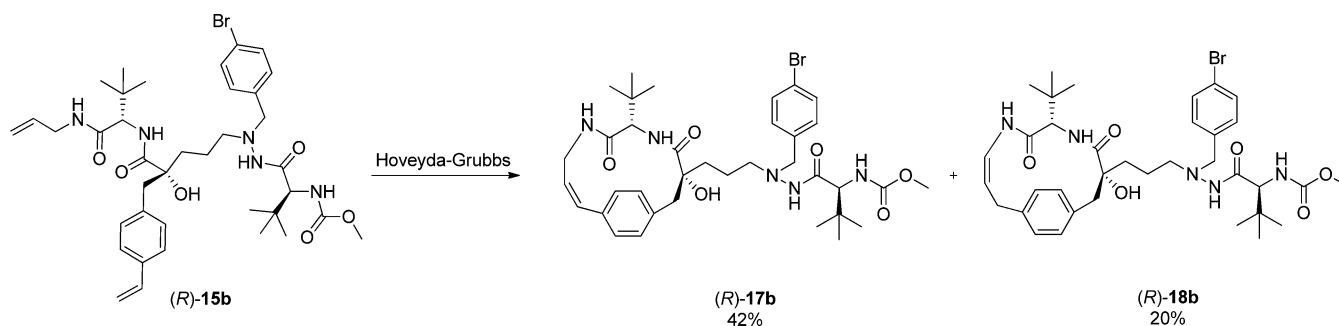
[a]Reagents and conditions: second-generation Hoveyda–Grubbs catalyst 10%, dry DCE, MW 130 °C, 1 h.

functionality was next engaged in a peptidic coupling with amine **8a–b** using HOBt and EDC. In each case, the obtained diastereoisomers (*R*)-**9** and (*S*)-**9** were easily separated by flash chromatography (Scheme 2). The absolute configuration specified refers to the asymmetric center of the lactone ring that was assigned on the basis of the solved X-ray structures of the final inhibitors (*R*)-**17b** (PDB code 3zps), (*R*)-**19a** (PDB code 3zpt), and (*R*)-**19b** (PDB code 3zpu) (Figure 3).

The lactone moiety of compounds (*R*)-**9a–b** and (*S*)-**9a–b** was reduced using LiBH$_4$. The newly formed primary alcohol

was selectively protected as a pivalate ester, and the tertiary alcohol was thereafter protected using *tert*-butyldimethylsilyl triflate (TBSOTf) in a stepwise manner. Deprotection of the primary alcohol using LiBH$_4$ provided compounds (*R*)-**10a-b** and (*S*)-**10a-b**. Introductions of different alkenes on the phenyl ring were next carried out. A vinyl group was attached via a microwave-induced Suzuki cross-coupling reaction[29,30] using palladium acetate as catalyst and 2,4,6-trivinylcyclotriboroxane pyridine complex as the alkene source,[31] giving (*R*)-**11a-b** and (*S*)-**11a-b**. The allyl group was introduced by microwave-

Scheme 5[a]

(R)-16a-b   (R)-19a-b
                                                36%
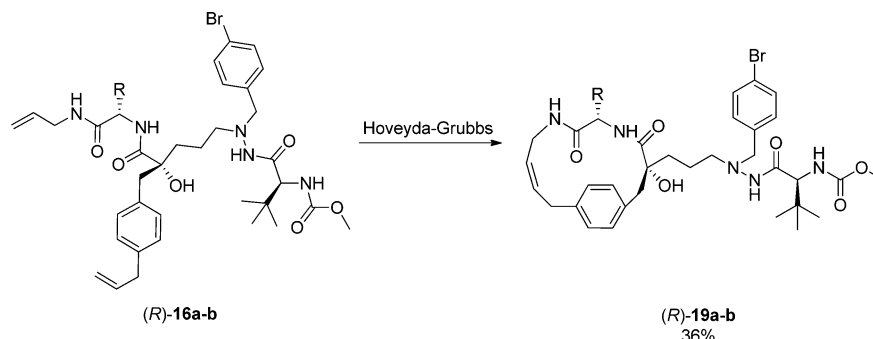
[a]Reagents and conditions: second-generation Hoveyda−Grubbs catalyst 10%, dry DCM, MW 60 °C, 30 min.

promoted Stille coupling using Pd(PPh$_3$)$_2$Cl$_2$ and allyltributyl-stannyl,[32] affording (R)-12a-b.

The primary alcohols were oxidized to aldehydes with Dess−Martin periodinane. A reductive amination with the previously reported hydrazide 13[19] was next conducted using NaBH-(OAc)$_3$ as the reducing agent. The tertiary alcohol group was then deprotected with TBAF (Scheme 3). In summary, 10 linear PIs were obtained using this synthetic route (Table 1).

The macrocyclization of compounds (R)-15b, (R)-16a, and (R)-16b were thereafter performed by microwave-induced ring-closing metathesis using the second-generation Hoveyda−Grubbs catalyst.[33] The macrocyclisation of the compound (R)-15b comprising a vinyl group gave two isolated 14-member ring isomers, (R)-17b (42%) and (R)-18b (20%), although enamide (R)-18b was found to be unstable over time (Scheme 4).

In the case of compounds (R)-16a and (R)-16b presenting an allyl group, only the 15-member ring compounds (R)-19a and (R)-19b were isolated (Scheme 5). Traces of isomers were detected by LC/MS but could not be purified. In all cases (17−19), the double bond of the macrocycle had a cis configuration according to NMR and X-ray structure analysis of cocrystallized inhibitor−enzyme complexes.

RESULTS AND DISCUSSION

Biological Results. The HIV-1 protease inhibition and cell-based antiviral activity of the 10 linear compounds were evaluated, and the corresponding K_i, EC$_{50}$, and CC$_{50}$ values are presented in Table 1.

All of the linear compounds with an R configuration of the tertiary alcohol display a strong inhibition profile (K_i between 10 and 37 nM), whereas compounds with those with an S configuration can be considered inactive with K_i values up to 100 times higher (K_i = 720−1000 nM). These results were expected from the results with our previous series of inhibitors.[14−18] The P2 4-aryl-elongated compounds (R)-15a, (R)-15b, (R)-16a, and (R)-16b displayed slightly higher K_i values compared to the parent structures (R)-14a and (R)-14b. Neither the cellular anti-HIV activity results (EC$_{50}$) nor the cytotoxic data (CC$_{50}$) showed a substantial difference between the linear active R compounds (EC$_{50}$ = 2.9−7.5 nM). Previously reported compound 20,[20] included in Table 2 for comparison, appears to be a better inhibitor (K_i = 2.7 nm, EC$_{50}$ = 2.1 μM) than all other linear compounds reported in this article. Compound 20 presents a nonsubstituted P1 benzyl group and a shorter P2 carbon chain than our new linear inhibitor series. However, the unsaturated P1 and P3 side chains in (R)-14−16 were primarily introduced to allow macrocyclization, furnishing (R)-17−19.

The macrocyclic compounds (results depicted in Table 2) furnish 2- to 3-fold better K_i values than the linear compounds. The results regarding compound (R)-18b are not communicated because degradation has been observed by the time of the biological evaluation.
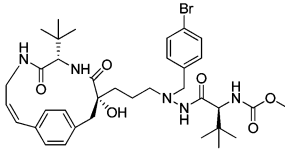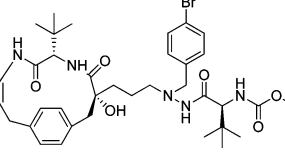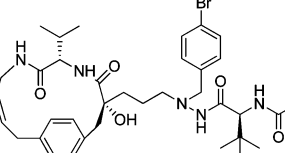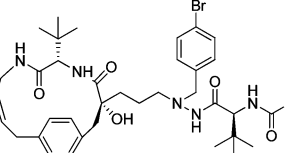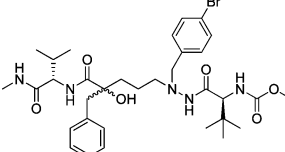
The cellular assay shows improvement in the EC$_{50}$ value for macrocyclic structures, especially for (R)-19a (EC$_{50}$ = 0.37 μM) and (R)-19b (EC$_{50}$ = 1.0 μM). In the case of (R)-19a, the cellular activity is 8 times better than the best linear compound, (R)-14b (EC$_{50}$ = 2.9 μM). Further, the cytotoxicity of the macrocyclic series seems to be somewhat lower than that of the linear series.

Values in Table 2 show that all macrocyclic compounds possess K_i and EC$_{50}$ values in the same range as compound 20. Interestingly, (R)-19a showed a similar K_i value as 20, whereas it exhibited a 6 times lower EC$_{50}$ value (0.37 vs 2.1 μM). The reduced apparent lipophilicity of the macrocyclic structure compared to the linear one could help explain this difference. Note that (R)-19a and (R)-19b combine low EC$_{50}$ values (0.37−1.0 μM) with satisfying permeability in the Caco-2 assay (P_{app} = 9−10 × 10^{-6} cm/s). In addition, linear PIs 15b, 16a, 16b also showed excellent permabilities (P_{app} > 40 × 10^{-6} cm/s).

X-ray Structure Analysis. The X-ray crystallography model of the arrangement of compounds (R)-17b (PDB code 3zps), (R)-19a (PDB code 3zpt), and (R)-19b (PDB code 3zpu) in the active site of the HIV-1 protease, including the most relevant hydrogen bonds to the enzyme amino acid residues, is presented in Figure 3 along with a previously published noncyclic compound 21 for comparison.[20] The new linear PIs exposed in this article, sadly, failed to give good crystallographic data. The protease complexes with compounds (R)-17b, (R)-19a, and (R)-19b were refined to data extending to 1.55, 1.54, and 1.80 Å, respectively. The compounds were easily traced, and the final R_{free} values of 21.0, 24.2, and 22.4%, respectively, as well the corresponding electron density maps suggest a good fit to the data.

Most hydrogen bond lengths are very similar for all three compounds, with hydrogen bonds between Asp25/125 and the tertiary alcohol oxygen being significant exceptions. Because these hydrogen bonds mimic the bonds formed during the catalytic reaction, the strength of these bonds is of particular interest. The most favored hydrogen bond to the tertiary alcohol oxygen is found in (R)-19a, with the shortest distance of 2.7 and 3.0 Å to the catalytic aspartic acids 125 and 25,

Table 2. Enzyme Inhibition Data, Antiviral Activity, and Cytotoxicity of Macrocyclic Tertiary-Alcohol-Comprising HIV-1 PIs

Compound	Structure	K_i (nM)	EC_{50} (µM)	CC_{50} (µM)	P_{app} ($\times 10^{-6}$ cm/s)
(R)-17b		5.0	3.3	40	31[b]
(R)-18b[a]		-	-	-	-
(R)-19a		3.1	0.37	>50	9[b], 29[c]
(R)-19b		4.2	1.0	30	10[b], 123[c]
20[20]		2.7	2.1	>10	

[a]Inhibitor (R)-18b decomposed before evaluation. [b]Measured Caco-2 permeabilities. [c]Predicted Caco-2 permeabilities (P_{app}) with the program QikProp (Schrödinger).

respectively. The corresponding bonds in the (R)-19b complex are weaker, with distances of 2.9 and 3.3 Å. Hydrogen bonds with a distance of more than about 3.2 Å between the donor and acceptor are usually considered weak, and hydrogen bonds with distances longer than 3.2 Å are mainly included here for comparison. In the (R)-17b complex, both of these bonds appear to be lost or considerably weaker. The corresponding distances between the carboxyl oxygen atoms in Asp125 and Asp25 are 3.2 and 3.4 Å, respectively, but the geometry is different. The carboxylic group of Asp125 is rotated toward the carboxylic group of Asp25, as compared to the arrangement in, for instance, complex (R)-19b. This indicates a stronger bond between the two carboxylic oxygens, with a distance between

oxygen atoms of 2.4 Å. As a result, the distance between the carboxyl group and the tertiary alcohol oxygen is 3.2 Å, and the bonding angle is less favorable for hydrogen bonding. In addition, Asp25 is shifted, resulting in a longer distance to the tertiary alcohol, 3.4 Å. Although the full mechanism behind the different geometry in the (R)-17b complex is not fully understood, a possible explanation is related to the slightly bulkier P1−P3 region of the more strained (R)-17b as compared to (R)-19b, which allows Gly27 to approach the compound site, resulting in a small rotation of Asp25. The fact the compounds are nonsymmetrical is reflected by the symmetry-related hydrogen-bond distances both to the two proteolytically active residues Asp25/125 and to the bonds
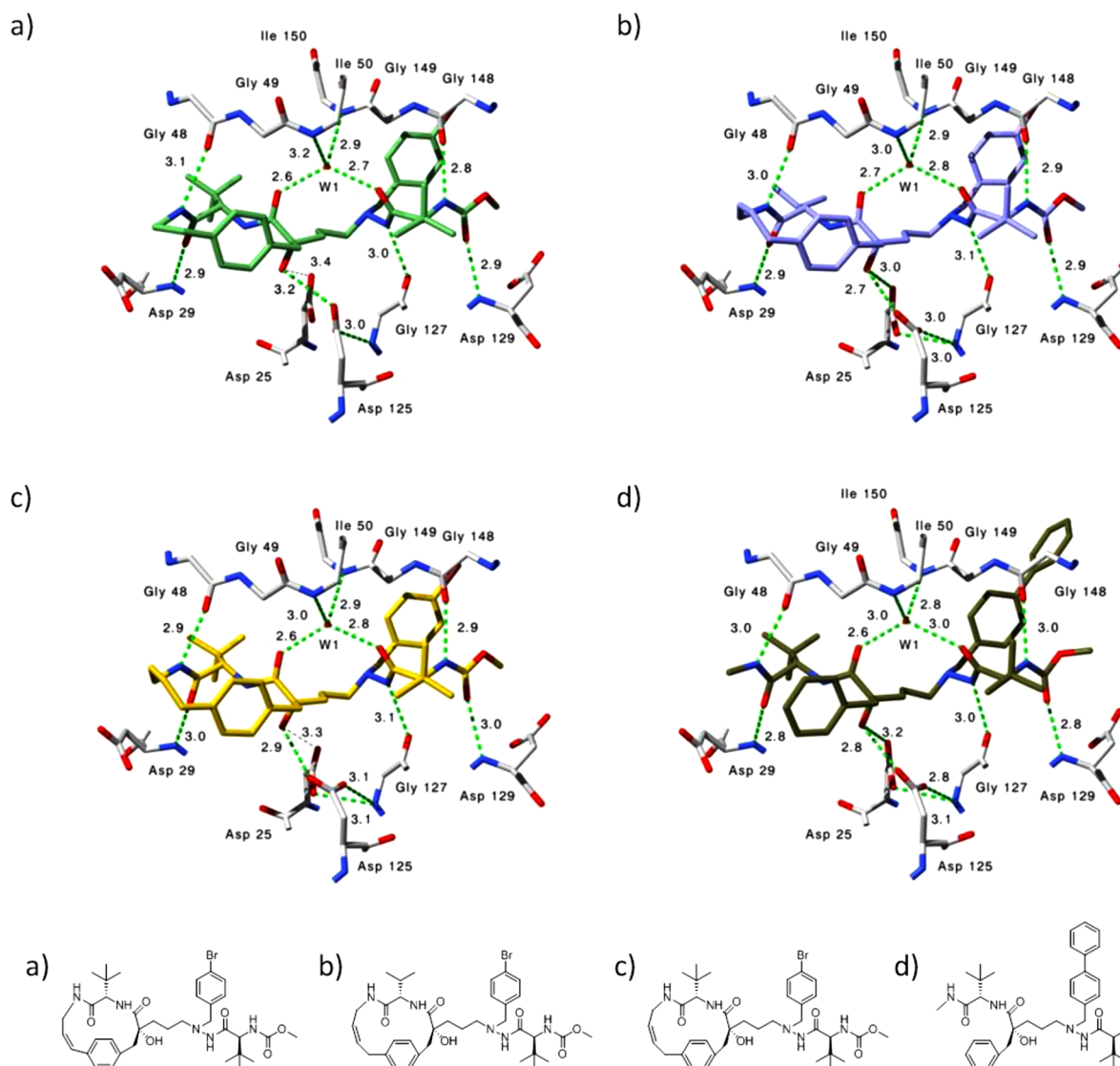
Figure 3. X-ray and chemical structures of the compounds (R)-**17b** (a; PDB code 3zps), (R)-**19a** (b; PDB code 3zpt), (R)-**19b** (c; PDB code 3zpu), and **21** (d; PDB code 2xye) cocrystallized with the HIV-1 protease. The arrangement in the active site is presented, and hydrogen bonds are shown with their bond distances.

between the compound and water W1 as well as between W1 and Ile50/150. For larger sized images of the X-ray structures, see the Supporting Information.

The hydrogen-bonding patterns differs between the (R)-**19a** and the (R)-**19b** complexes as a result of the bulkier t-butyl group of compound (R)-**19b** as compared to the corresponding isopropyl group of compound (R)-**19a**. In the (R)-**19b** complex, amino acids Ala28, Asp29, and Asp30 shift their position to avoid having too close of contact with the inhibitor. This causes the entire circular structure to rotate along the longest axes of the compound (Figure 4). The effect is a small shift of the tertiary alcohol group, resulting in the slightly longer H-bond distances in compound (R)-**19b**, as seen in Figure 1.

Comparisons between macrocycles (R)-**17b**, (R)-**19a**, (R)-**19b** and noncyclic compound **21** are presented in Figure 5. The macrocyclic structures mimic the binding geometry of linear inhibitor **21** very well. The one-carbon-smaller ring of structure (R)-**17b** as compared to compounds (R)-**19a** and (R)-**19b** seem to make the ring more strained with less favorable angles, resulting in a different local geometry,

although the two ring structures superimpose well, and the effect on the overall binding is small. The linker added to close the macrocycle is hydrophobic. The region is exposed to the surface as well as to the hydrophilic side chains of Arg108, which may suggest that a more hydrophilic linker that would be able to facilitate a similar geometry could further improve the binding.

■ CONCLUSIONS

Thirteen novel HIV-1 protease inhibitors have been synthesized. Three macrocyclic compounds were obtained by 14- and 15-member P1−P3 macrocyclizations of a previously reported series of HIV-1 protease inhibitors that encompasses a tertiary alcohol as part of the transition-state-mimicking scaffold. Up to 15 times more potent cyclic compounds were obtained, exhibiting EC_{50} values down to 0.37 μM. In all cases, the macrocycles were more potent than the open-chain equivalents, but the difference in potency was not dramatic, suggesting that the N-terminus and the vinyl and the allylic group in the P1 para position partly accommodate the same space as the
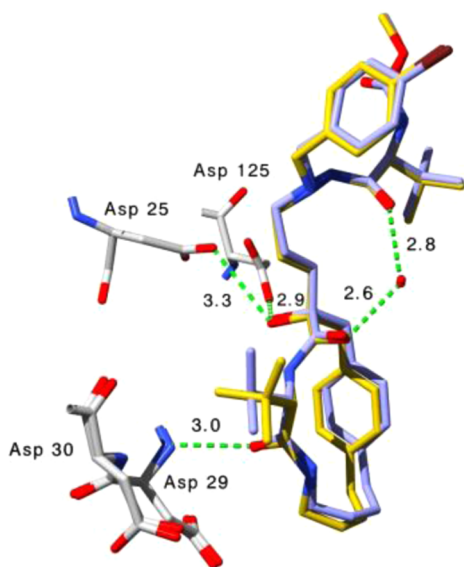
Figure 4. Structure of the complex with (R)-**19a** (gray) superimposed on the (R)-**19b** complex (gold) (viewed from above-front as compared to Figure 3).
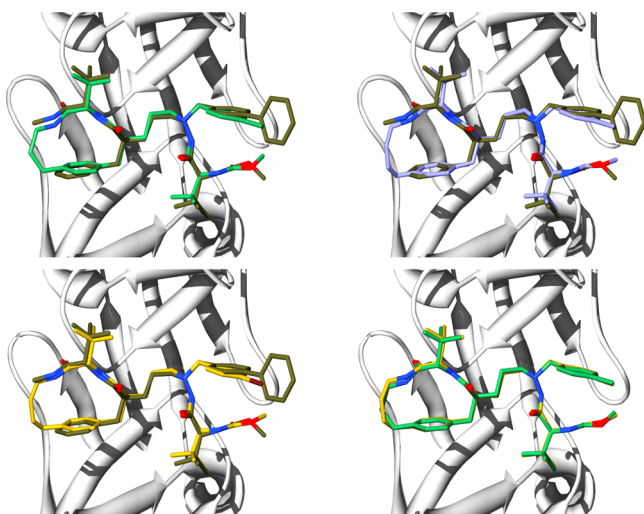

Figure 5. Comparison between the complexes of compounds (R)-**17b** (green) and noncyclic compound **21** (brown) (top left), (R)-**19a** (purple) and **20** (brown) (top right), and (R)-**19b** (gold) and **21** (brown) (bottom left) as well as between the 15-member ring (R)-**19b** (gold) and the 14-member ring (R)-**17b** (green) (bottom right).

lipophilic linker, mimicking P1−P3. X-ray crystallographic data analyses of three cocrystallized inhibitor−enzyme complexes provide a good understanding of the binding mode for the macrocyclic inhibitors. The reported HIV-1 protease inhibitors will serve as leads for further optimization by elongation in the P1′ position.

■ EXPERIMENTAL SECTION

General Methods. ^1H and ^{13}C NMR spectra were recorded on Varian Mercury Plus instruments: ^1H at 399.9 MHz and ^{13}C at 100.6 MHz at 25 °C. Analytical RPHPLC-MS was performed on a Gilson HPLC system with a Finnigan AQA quadrupole low-resolution mass spectrometer in positive or negative ESI mode using a Onyx Monolithic C$_{18}$ 4.6 × 50 mm, 5 μm (Phenomenex) or ACT C4 4.6 × 50 mm, 5 μm column with MeCN in 0.05% aqueous HCOOH as the mobile phase at a flow rate of 4 mL/min. Preparative RPLC-MS

was performed on a Gilson HPLC system using a Zorbax SB-C8, 5 μm, 21.2 × 150 mm (Agilent technologies) column, with MeCN in 0.05% aqueous HCOOH as the mobile phase at a flow rate of 10−15 mL/min or with MeCN in 0.1% aqueous TFA as the mobile phase at a flow rate of 5 mL/min. Exact molecular masses were determined on Micromass Q-Tof2 mass spectrometer equipped with an electrospray ion source. Optical rotations were obtained on a PerkinElmer 241 polarimeter, specific rotations ($[\alpha]_D$) are reported in deg/dm, and the concentration (c) is given in g/100 mL in the specified solvent. All protease inhibitors were >95% pure according to ^1H NMR, LC-UV (254 nm and 214 or 220 nm), and LC-MS (TIC).

Procedure and Spectroscopic Data for Macrocyclic Compounds (R)-17b−(R)-19b. *(R)-17b and (R)-18b.* A 0.5−2.0 mL microwave vial was charged with (R)-**15b** (15 mg, 1.2 mmol) and Hoveyda−Grubbs second-generation catalyst (10 mol %) in 1,2-dichloroethane (3 mL) and irradiated in the microwave reactor cavity at 130 °C for 1 h. The reaction mixture was passed through a short Celite plug, and the plug was rinsed with EtOAc (15 mL). The organic layer was washed with brine (2 × 15 mL), dried over Na$_2$SO$_4$, and concentrated under reduced pressure. Preparative HPLC purification yielded (R)-**17b** (5 mg, 42% yield) and (R)-**18b** (3 mg, 20% yield) as light-brown oils that were freeze-dried. For (R)-**17b**, ^1H NMR (400 MHz, CDCl$_3$): δ 7.34−7.51 (m, 3H), 6.93−7.17 (m, 8H), 6.12−6.16 (m, 1H), 6.31 (dd, J = 14.4, 15.6 Hz, 1H), 5.63 (d, J = 10.8 Hz, 1H), 5.05−5.13 (m, 1H), 3.67−4.03 (m, 3H), 3.58 (s, 3H), 3.26−3.43 (m, 2H), 2.55−3.01 (m, 4H), 1.98−2.34 (m, 4H), 1.80 (d, J = 6.4 Hz, 1H), 0.67−1.01 (m, 18H). ^{13}C NMR (100 MHz, CDCl$_3$): δ 18.7, 26.5, 27.0, 27.3, 33.9, 35.4, 36.5, 42.1, 45.7, 52.8, 57.0, 60.4, 61.5, 66.7, 68.2, 79.8, 121.8, 125.7, 128.6, 129.6, 130.8, 131.0, 131.4, 131.8, 135.0, 135.9, 137.9, 156.9, 167.8, 171.1, 174.6. HRMS m/z: [M + H$^+$] calcd for C$_{36}$H$_{50}$BrN$_5$O$_6$, 728.3023; found, 728.3021. For (R)-**18b**, ^1H NMR (400 MHz, CDCl$_3$): δ 6.98−7.47 (m, 8H), 6.76−7.03 (m, 1H), 6.29 (d, J = 16.4 Hz, 1H), 5.09−5.15 (m, 1H), 3.70−3.93 (m, 4H), 3.57 (s, 3H), 3.24−3.47 (m, 2H), 3.01−3.08 (m, 1H), 2.69−2.80 (m, 3H), 2.11−2.42 (m, 4H), 1.57−1.84 (m, 4H), 0.64−1.41 (m, 18H). ^{13}C NMR (100 MHz, CDCl$_3$): δ 21.2, 22.5, 26.5, 26.9, 29.5, 33.9, 35.3, 36.5, 42.1, 46.2, 52.8, 57.4, 60.3, 61.9, 66.8, 68.4, 79.7, 103.8, 121.9, 123.1, 125.9, 126.4, 128.2, 130.8, 131.4, 131.7, 136.3, 137.2, 139.3, 157.3, 158.4, 167.1, 177.5. HRMS m/z: [M + H$^+$] calcd for C$_{36}$H$_{50}$BrN$_5$O$_6$, 728.3023; found, 728.3027.

(R)-19a. A 10−20 mL microwave vial was charged with (R)-**16a** (24 mg, 0.32 mmol) and Hoveyda−Grubbs second-generation catalyst (10 mol %) in DCM (9 mL) and irradiated in the microwave reactor cavity at 60 °C for 30 min. The reaction mixture was passed through a short Celite plug, and the plug was rinsed with EtOAc (15 mL). The organic layer was concentrated under reduced pressure. Preparative HPLC purification yielded (R)-**19a** (8 mg, 35% yield) as a colorless oil. ^1H NMR (400 MHz, CD$_3$OD): δ 7.44−7.36 (m, 2H), 7.30 (m, 3H), 7.07 (m, 2H), 6.87 (m, 1H), 6.32 (dt, J = 10.2, 7.4 Hz, 1H), 5.70 (td, J = 10.2, 7.6 Hz, 1H), 3.93−3.81 (m, 3H), 3.75−3.66 (m, 2H), 3.63 (s, 3H), 3.48−3.33 (m, 2H), 2.80 (m, 4H), 2.03 (m, 1H), 1.87 (m, 2H), 1.72 (m, 1H), 1.48 (m, 1H), 1.30 (m, 3H), 0.83−0.71 (m, 15H). ^{13}C NMR (101 MHz, CD$_3$OD): δ 176.15, 172.23, 172.07, 142.49, 137.87, 136.38, 135.47, 132.60, 132.37, 131.55, 131.22, 129.47, 129.38, 128.30, 122.31, 80.57, 63.15, 62.18, 59.51, 58.86, 56.20, 52.95, 47.14, 38.25, 37.61, 35.04, 32.97, 32.31, 32.24, 29.68, 27.05, 22.72, 19.82, 18.58. HRMS m/z: [M + H$^+$] calcd for C$_{36}$H$_{50}$BrN$_5$O$_6$, 728.3023; found, 728.3002.

(R)-19b. A microwave vial was charged with (R)-**16b** (15 mg, 0.19 mmol) and Hoveyda−Grubbs second-generation catalyst (10 mol %) in DCM (3 mL) and irradiated in the microwave reactor cavity at 60 °C for 30 min. The reaction mixture was passed through a short Celite plug, and the plug was rinsed with EtOAc (15 mL). The organic layer was concentrated under reduced pressure. Preparative HPLC purification yielded (R)-**19b** (5 mg, 36% yield) as a colorless oil. ^1H NMR (400 MHz, CD$_3$OD): δ 7.40 (m, 2H), 7.31 (m, 2H), 7.21 (m, 1H), 7.06 (dd, J = 7.9, 1.9 Hz, 1H), 6.97 (dd, J = 8.0, 1.9 Hz, 1H), 6.83 (dd, J = 7.9, 1.9 Hz, 1H), 6.30 (ddd, J = 10.4, 8.3, 6.6 Hz, 1H), 5.79 (ddt, J = 8.9, 6.2, 4.4 Hz, 1H), 4.04 (m, 1H), 3.85 (s, 2H), 3.71 (s, 1H), 3.62 (m, 4H), 3.49−3.32 (m, 2H), 3.12−3.02 (m, 1H), 2.89−

2.74 (m, 4H), 2.09−1.96 (m, 1H), 1.86 (m, 1H), 1.73 (m, 1H), 1.48 (m, 1H), 1.35−1.22 (m, 3H), 0.81 (m, 18H). ^{13}C NMR (101 MHz, CD$_3$OD): δ 175.77, 172.08, 170.85, 159.09, 141.63, 137.88, 135.81, 135.18, 132.62, 132.36, 131.26, 130.89, 129.44, 128.89, 128.36, 122.31, 80.61, 63.15, 62.16, 61.41, 58.89, 52.95, 38.07, 37.43, 35.87, 35.06, 32.78, 30.90, 29.69, 27.19, 27.07, 22.73. HRMS m/z: [M + H$^+$] calcd for C$_{37}$H$_{52}$BrN$_5$O$_6$, 742.3179; found, 742.3180

ASSOCIATED CONTENT

ⓢ Supporting Information

Experimental details and spectroscopic data for compounds **2**−(R)-**19b**; X-ray images and structure determination details. This material is available free of charge via the Internet at http://pubs.acs.org.

AUTHOR INFORMATION

Corresponding Author

*Phone: +46 184714667. Fax: +46 184714474. E-mail: Mats. Larhed@orgfarm.uu.se.

Author Contributions

‖These author contributed equally to this work.

Notes

The authors declare no competing financial interest.

ACKNOWLEDGMENTS

ABBREVIATIONS USED

AIDS, acquired immune deficiency syndrome; EDC, 1-(3-dimethylaminopropyl)-3-ethylcarbodiimide hydrochloride; HAART, highly active antiretroviral therapy; HIV, human immunodeficiency virus; HOBt, 1-hydroxybenzotriazole; PDB, Protein Data Bank; PI, protease inhibitor; WHO, World Health Organization; MW, microwaves

REFERENCES

(1) Mastrolorenzo, A.; Rusconi, S.; Scozzafava, A.; Barbaro, G.; Supuran, C. T. Inhibitors of HIV-1 protease: Current state of the art 10 years after their introduction. From antiretroviral drugs to antifungal, antibacterial and antitumor agents based on aspartic protease inhibitors. *Curr. Med. Chem.* **2007**, *14*, 2734−2748.

(2) Hawkins, T. Understanding and managing the adverse effects of antiretroviral therapy. *Antiviral Res.* **2010**, *85*, 201−209.

(3) FDA list of antiretroviral drugs used in the treatment of HIV infection. http://www.fda.gov/ForConsumers/byAudience/ForPatientAdvocates/HIVandAIDSActivities/ucm118915.htm

(4) Mangum, E. M.; Graham, K. K. Lopinavir−Ritonavir: A new protease inhibitor. *Pharmacotherapy* **2001**, *21*, 1352−1363.

(5) Temesgen, Z.; Cainelli, F.; Vento, S. Tipranavir. *Drugs Today* **2005**, *41*, 711−720.

(6) Randolph, J. T.; DeGoey, D. A. Peptidomimetic inhibitors of HIV protease. *Curr. Top. Med. Chem.* **2004**, *4*, 1079−1095.

(7) Rodriguez-Barrios, F.; Gago, F. HIV protease inhibition: Limited recent progress and advances in understanding current pitfalls. *Curr. Top. Med. Chem.* **2004**, *4*, 991−1007.

(8) Clavel, F.; Hance, A. J. HIV drug resistance. *N. Engl. J. Med.* **2004**, *350*, 1023−1035.

(9) Taylor, B. S.; Hunt, G.; Abrams, E. J.; Coovadia, A.; Meyers, T.; Sherman, G.; Strehlau, R.; Morris, L.; Kuhn, L. Rapid development of antiretroviral drug resistance mutations in HIV-infected children less than two years of age initiating protease inhibitor-based therapy in South Africa. *AIDS Res. Hum. Retroviruses* **2011**, *27*, 945−956.

(10) Croom, K. F.; Dhillon, S.; Keam, S. J. Atazanavir: A review of its use in the management of HIV-1 infection. *Drugs* **2009**, *69*, 1107−1140.

(11) Wang, F.; Ross, J. Atazanavir: A novel azapeptide inhibitor of HIV-1 protease. *Formulary* **2003**, *38*, 691−702.

(12) Kim, R.; Baxter, J. D. Protease inhibitor resistance update: Where are we now? *AIDS Patient Care STDs* **2008**, *22*, 267−277.

(13) Colonno, R.; Rose, R.; McLaren, C.; Thiry, A.; Parkin, N.; Friborg, J. Identification of I50L as the signature atazanavir (ATV)-resistance mutation in treatment-naive HIV-1-infected patients receiving ATV-containing regimens. *J. Infect. Dis.* **2004**, *189*, 1802−1810.

(14) Ekegren, J. K.; Unge, T.; Safa, M. Z.; Wallberg, H.; Samuelsson, B.; Hallberg, A. A new class of HIV-1 protease inhibitors containing a tertiary alcohol in the transition-state mimicking scaffold. *J. Med. Chem.* **2005**, *48*, 8098−8102.

(15) Ekegren, J. K.; Ginman, N.; Johansson, A.; Wallberg, H.; Larhed, M.; Samuelsson, B.; Unge, T.; Hallberg, A. Microwave-accelerated synthesis of P1′-extended HIV-1 protease inhibitors encompassing a tertiary alcohol in the transition-state mimicking scaffold. *J. Med. Chem.* **2006**, *49*, 1828−1832.

(16) Ekegren, J. K.; Gising, J.; Wallberg, H.; Larhed, M.; Samuelsson, B.; Hallberg, A. Variations of the P2 group in HIV-1 protease inhibitors containing a tertiary alcohol in the transition-state mimicking scaffold. *Org. Biomol. Chem.* **2006**, *4*, 3040−3043.

(17) Mahalingam, A. K.; Axelsson, L.; Ekegren, J. K.; Wannberg, J.; Kihlstrom, J.; Unge, T.; Wallberg, H.; Samuelsson, B.; Larhed, M.; Hallberg, A. HIV-1 protease inhibitors with a transition-state mimic comprising a tertiary alcohol: Improved antiviral activity in cells. *J. Med. Chem.* **2010**, *53*, 607−615.

(18) Wu, X.; Ohrngren, P.; Ekegren, J. K.; Unge, J.; Unge, T.; Wallberg, H.; Samuelsson, B.; Hallberg, A.; Larhed, M. Two-carbon-elongated HIV-1 protease inhibitors with a tertiary-alcohol-containing transition-state mimic. *J. Med. Chem.* **2008**, *51*, 1053−1057.

(19) Wu, X.; Ohrngren, P.; Joshi, A. A.; Trejos, A.; Persson, M.; Arvela, R. K.; Wallberg, H.; Vrang, L.; Rosenquist, A.; Samuelsson, B. B.; Unge, J.; Larhed, M. Synthesis, X-ray analysis, and biological evaluation of a new class of stereopure lactam-based HIV-1 protease inhibitors. *J. Med. Chem.* **2012**, *55*, 2724−2736.

(20) Ohrngren, P.; Wu, X. Y.; Persson, M.; Ekegren, J. K.; Wallberg, H.; Vrang, L.; Rosenquist, A.; Samuelsson, B.; Unge, T.; Larhed, M. HIV-1 protease inhibitors with a tertiary alcohol containing transition-state mimic and various P2 and P1′ substituents. *MedChemComm* **2011**, *2*, 701−709.

(21) Rich, D. H. Pepstatin-derived inhibitors of aspartic proteinases. A close look at an apparent transition-state analogue inhibitor. *J. Med. Chem.* **1985**, *28*, 263−273.

(22) Kim, B. M.; Guare, J. P.; Hanifin, C. M.; Arfordbickerstaff, D. J.; Vacca, J. P.; Ball, R. G. A convergent synthesis novel conformationally restricted Hiv-1 protease inhibitors. *Tetrahedron Lett.* **1994**, *35*, 5153−5156.

(23) Driggers, E. M.; Hale, S. P.; Lee, J.; Terrett, N. K. The exploration of macrocycles for drug discovery − an underexploited structural class. *Nat. Rev. Drug Discovery* **2008**, *7*, 608−624.

(24) Marsault, E.; Peterson, M. L. Macrocycles are great cycles: Applications, opportunities, and challenges of synthetic macrocycles in drug discovery. *J. Med. Chem.* **2011**, *54*, 1961−2004.

(25) Podlogar, B. L.; Farr, R. A.; Friedrich, D.; Tarnus, C.; Huber, E. W.; Cregge, R. J.; Schirlin, D. Design, synthesis, and conformational analysis of a novel macrocyclic HIV-protease inhibitor. *J. Med. Chem.* **1994**, *37*, 3684−3692.

(26) Janetka, J. W.; Raman, P.; Satyshur, K.; Flentke, G. R.; Rich, D. H. Novel cyclic biphenyl ether peptide beta-strand mimetics and HIV-protease inhibitors. *J. Am. Chem. Soc.* **1997**, *119*, 441−442.

(27) Ghosh, A. K.; Kulkarni, S.; Anderson, D. D.; Hong, L.; Baldridge, A.; Wang, Y. F.; Chumanevich, A. A.; Kovalevsky, A. Y.; Tojo, Y.; Amano, M.; Koh, Y.; Tang, J.; Weber, I. T.; Mitsuya, H. Design, synthesis, protein-ligand X-ray structure, and biological evaluation of a series of novel macrocyclic human immunodeficiency

virus-1 protease inhibitors to combat drug resistance. *J. Med. Chem.* **2009**, *52*, 7689−7705.

(28) Tojo, Y.; Koh, Y.; Amano, M.; Aoki, M.; Das, D.; Kulkarni, S.; Anderson, D. D.; Ghosh, A. K.; Mitsuya, H. Novel protease inhibitors (PIs) containing macrocyclic components and 3(*R*),3a(*S*),6a(*R*)-bis-tetrahydrofuranylurethane that are potent against multi-PI-resistant HIV-1 variants in vitro. *Antimicrob. Agents Chemother.* **2010**, *54*, 3460−3470.

(29) Noteberg, D.; Schaal, W.; Hamelink, E.; Vrang, L.; Larhed, M. High-speed optimization of inhibitors of the malarial proteases plasmepsin I and II. *J. Comb. Chem.* **2003**, *5*, 456−64.

(30) Gising, J.; Odell, L. R.; Larhed, M. Microwave-assisted synthesis of small molecules targeting the infectious diseases tuberculosis, HIV/AIDS, malaria and hepatitis C. *Org. Biomol. Chem.* **2012**, *10*, 2713−2729.

(31) Wannberg, J.; Sabnis, Y. A.; Vrang, L.; Samuelsson, B.; Karlen, A.; Hallberg, A.; Larhed, M. A new structural theme in C2-symmetric HIV-1 protease inhibitors: Ortho-substituted P1/P1′ side chains. *Bioorg. Med. Chem.* **2006**, *14*, 5303−5315.

(32) Larhed, M.; Hoshino, M.; Hadida, S.; Curran, D. P.; Hallberg, A. Rapid fluorous Stille coupling reactions conducted under microwave irradiation. *J. Org. Chem.* **1997**, *62*, 5583−5587.

(33) Coquerel, Y.; Rodriguez, J. Microwave-assisted olefin metathesis. *Eur. J. Org. Chem.* **2008**, *7*, 1125−1132.